Power-law scaling in human EEG:

Moment analysis and clinical stroke detection

*T. C. Ferree[1] and R. C. Hwa[2]

[1] Dynamic Neuroimaging Laboratory, Department of Radiology, University of California San Francisco

[2] Institute of Theoretical Science and Department of Physics, University of Oregon

February 7, 2002

Abstract

It has recently been demonstrated that human resting EEG time series exhibit power-law scaling behavior typically over two temporal ranges [1]. The scaling exponents provide a concise description of the complex nonlinear fluctuations without assuming low-dimensional chaotic attractors. This paper extends that analysis to consider the fluctuations over the 128 scalp electrodes. It shows that the moments of the temporal scaling exponents also exhibit power-law behavior, such that the entire spatiotemporal data set may be characterized in just a few parameters. These global scaling parameters discriminate remarkably well between normal subjects and those with cerebral ischemic stroke.

Keywords: Electroencephalography, power-law, scaling, complexity, stroke.

PREPRINT

Submitted to 2002 Computational Neuroscience Meeting

*Corresponding author. Telephone: (415) 502-3726; Email: tom.ferree@radiology.ucsf.edu

1 Introduction

In a companion paper [1], we have presented the results of a nonlinear analysis of resting EEG time series. Using the method of detrended fluctuation analysis (DFA), we have found that a fluctuation measure $F(k)$ over a time interval k exhibits power-law scaling behavior

$$F(k) \propto k^{\alpha} \tag{1}$$

over two regions of k, resulting in two scaling exponents α_1 and α_2. This behavior is found to hold in nearly all channels and all subject examined. For details the reader is referred to Ref. [1]. The focus of this paper is to consider the fluctuations of the scaling exponents across multiple electrodes, and address the question of what one can learn from these scaling exponents.

The EEG used in our study consists of 128 channels distributed over the scalp, each characterized by two scaling exponents α_i, where $i = 1, 2$. An open challenge is how best to represent the spatial variability. The most common procedure would be to plot the scaling exponents topographically and seek anatomical correlates, but this presumes that the interesting features are spatially focal, which may not be the case given the existence of long-range connections throughout the cortex [6]. Here we seek a global description which is the counterpart of the temporal analysis in [1].

It is tempting to try to study spatial scaling behavior, but this is not possible for scalp EEG because the resolution is inadequate to allow the study of fluctuations on spatial scales differing by decades. Instead, our approach is to study the distributions of the α_i over the scalp, ignoring their spatial relationships initially, and emphasizing instead the global structure of the α_i values themselves. We find that these moments also obey power-law scaling behavior [4]. This allows further summarization of the data, and provides a concise description of global brain state.

We apply these techniques to clinical stroke detection. Cerebral ischemic stroke is one example where it has been shown that the effects of a focal blood flow reduction may have nonfocal effects on the EEG [5]. We find that, via moment analysis, a global dynamical measure can be constructed which is capable of distinguishing normal from stroke subjects.

2 Moment analysis

Before describing our approach, let us first see how the values of (α_1, α_2) are distributed. Figure 1a shows a scatter plot of the values of α_2 versus α_1 for an arbitrarily chosen subject A. Each channel contributes one point to the plot. Evidently, both values are widely distributed and with rare exceptions the value of α_1 is always larger than the value of the companion α_2 at the same channel. That is not to say that α_1 of one channel cannot be smaller than α_2 of another channel. Our problem is to find a method to represent these 128 pairs of α exponents in a succinct way.

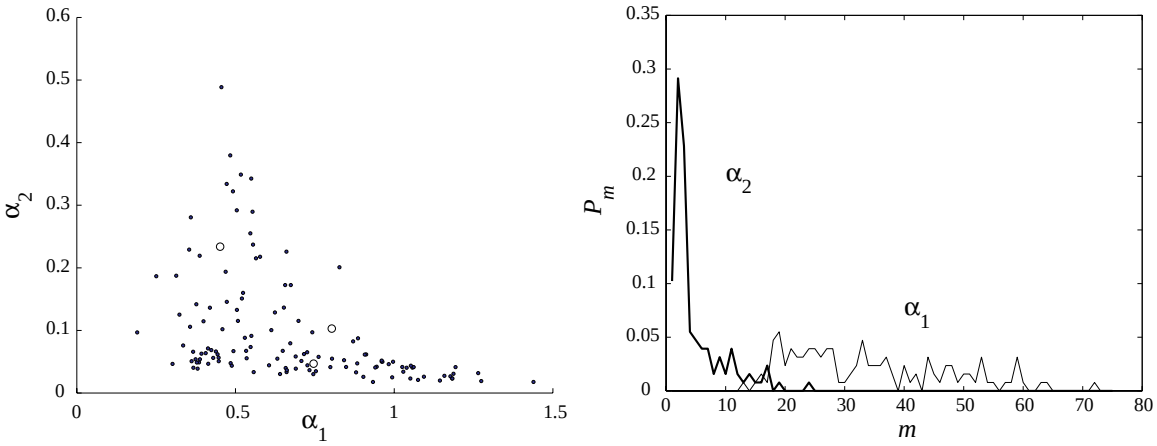

Figure 1: Distributions of scaling exponents: (a) scatter plot, and (b) histogram. The open circles in (a) represent the three channels studied in Ref. [1].

To this end, we propose to consider the statistical moments of the scaling exponents. Since the distributions in Fig. 1a are not Gaussian, the mean and variance alone will not suffice. In general, if we have N numbers, z_j, where $j = 1, \cdots, N$, we can calculate arbitrarily many moments

$$G_q = \frac{1}{N} \sum_{j=1}^{N} z_j^q, \tag{2}$$

where q is a positive integer [2]. The information contained in the first N moments (i.e., $q = 1, \cdots, N$) is enough to reproduce all the z_j by inversion. However, for the sake of economy in extracting information we may find that only a few of the G_q with lower order q may be sufficient, since each of them contains some information of all the z_j. In our present problem we have $N = 128$, and we shall consider the first ten orders, $1 \leq q \leq 10$. That is a significant reduction of numbers, a process

worth investigating.

The moments are the weighted averages of the probability distributions of α_1 and α_2. A visualization of those distributions can be achieved by making projections of the points in Fig. 1a onto the α_1 and α_2 axes. Let x be either α_1 or α_2. Since no value of α_i has been found to exceed 1.5 in the subjects we have examined, we consider the interval $0 \leq x \leq 1.5$. Divide that interval into M equal cells, which for definiteness we take to be $M = 150$ here. Let the cells be labeled by $m = 1, \cdots, M$, each having the size $\delta x = 1.5/M$. Denote the number of channels whose x values are in the mth cell by n_m. Define

$$P_m = n_m \,/\, N. \tag{3}$$

It is the fraction of channels whose x values are in the range $(m-1)\,\delta x \leq x < m\,\delta x$. By definition, we have $\sum_{m=1}^{M} P_m = 1$. Fig. 1b shows the two distributions P_m for subject A. G_1 gives the average, and G_2 is related to the width.

Since the variance and other moments typically increase monotonically with the mean of a distribution, the fluctuation of m in P_m is best measured relative to its mean. Let us therefore consider the normalized moments [3]

$$M_q^{(i)} = G_q^{(i)} \Big/ \left(G_1^{(i)}\right)^q = \sum_{m=1}^{M} m^q P_m^{(i)} \Big/ \left(\sum_{m=1}^{M} m P_m^{(i)}\right)^q, \tag{4}$$

where $i = 1$ or 2. Since these moments are averages of $(m/\overline{m})^q$, where $\overline{m}$ is the average-m, they are not very sensitive to $\overline{m}$ itself. Together they contain the majority of the statistical information about the fluctuation properties of $\alpha_{1,2}$ in all channels.

In Fig. 2a the q-dependences of $\ln\, M_q^{(1,2)}$ are shown for $2 \leq q \leq 10$, for the distributions exhibited in Fig. 1b. They are approximately linear except for the low values of q, as shown by the two straight lines that fit very well the behaviors for $q \geq 5$. The same type of dependencies on q are found for all subjects. Thus for large q we have

$$\ln M_q^{(i)} \propto \mu_i\, q, \qquad q \geq 5. \tag{5}$$

Because they are defined for the higher moments $q \geq 5$, the parameters μ_i are particularly sensitive to the tails of the distributions $P_m^{(i)}$ of the α_i.

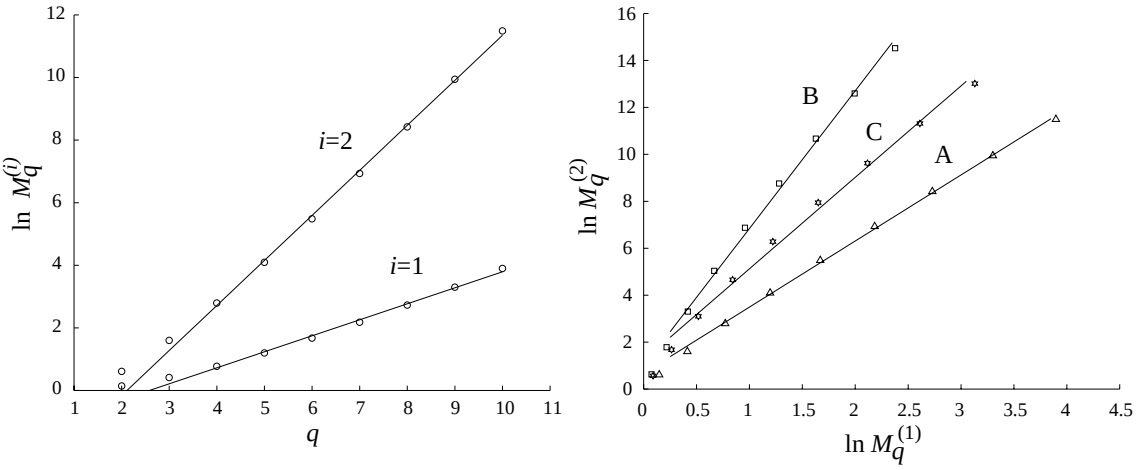

Figure 2: Power-law behavior of moments: (a) q-dependence of $\ln M_q^{(1,2)}$ for subject A, (b) $\ln M_q^{(1)}$ versus $\ln M_q^{(2)}$ for three subjects.

An even further summarization of these data is possible, which relates the moments of the distributions of the two scaling exponents α_1 and α_2. Visual extrapolations of the lines in Fig. 2a to lower values of q show the degree of deviation of the values of $\ln M_q^{(1,2)}$ from linearity. Since $\ln M_q^{(1)}$ and $\ln M_q^{(2)}$ behave so similarly in their departures from their linear dependencies on q, and in order to exhibit their relationship directly without explicit dependence on q, we plot $\ln M_q^{(2)}$ versus $\ln M_q^{(1)}$. We find that they are linearly related over a much wider range of values. Remarkably this is found to be true for all subjects examined. The plots for three subjects are illustrated in Fig. 2b. Thus the implication is that there exists a universal power-law behavior

$$M_q^{(2)} \propto \left(M_q^{(1)} \right)^{\eta} \tag{6}$$

valid for all subjects examined. From Eqs. (5) and (6) we obtain

$$\eta = \mu_2/\mu_1, \tag{7}$$

but now η is meaningful for all q (except for the lowest points) and in that sense independent of q. Thus we have discovered a single scaling exponent η that characterizes all α_i values of a subject, and varies from subject to subject. A study of the values of η for the resting EEG of 18 normal subjects has been carried out in Ref. [4]. It is found that they are well distributed over a range from 0.5 to 6.

The power-law behavior of Eq. (6) implies that the exponent η is independent of q, and that all α_i values are relevant contributors to the universal behavior. This is an important point worth emphasizing. The value η, although incredibly concise, carries a wealth of dynamical information. From a dynamical perspective, the value of η may be considered a parameterization of global brain state. It summarizes the spatial variability of the temporal scaling exponents $\alpha_{1,2}$ computed over short and long time scales. It remains to be seen how this global parameter changes as a function of brain state defined in terms of behavior, perception, etc.

Returning to Fig. 2a, the exponential fits with μ_1 and μ_2 do a good job of characterizing the large values of q, which are governed mostly by the values of (α_1, α_2) in the tails of the distributions shown in Fig. 1b. To capture the behaviors at low q, we consider the derivative of $\ln M_q^{(i)}$ at $q = 1$, which is at the opposite end of the range of q values from those in Eq.(5).

$$\sigma_i = \left. \frac{d}{dq} \ln M_q^{(i)} \right|_{q=1} = \sum_{m=1}^{M} P_m^{(i)} \left[\frac{m}{\overline{m}} \ln \frac{m}{\overline{m}} \right], \tag{8}$$

where in the second equality we made use of the fact that $M_q^{(i)} = 1$ at $q = 1$. This quantity is more sensitive to the fluctuations of m around the mean $\overline{m}$. Thus for each subject we can compute four parameters: (μ_1, μ_2) and (σ_1, σ_2), which more completely characterize the distributions $P_m^{(i)}$ in Fig. 1b for each subject.

3 Clinical stroke detection

We next apply the DFA and moment analyses to the problem of clinical stroke detection. Summary statistics have obvious utility in clinical diagnosis, where it is necessary to reduce the enormous amount of information coming from 128-channel EEG. We investigate whether the four scaling parameters (μ_1, μ_2) and (σ_1, σ_2) can distinguish between normal and stroke subjects.

Ten seconds of EEG data were collected from each of 10 subjects, resting with eyes closed, exactly as for the 18 control subjects discussed in Ref. [4]. For the various subjects, the data collection times ranged from a few hours to a few days after stroke onset. Thus the data range from acute to subacute, and we expect the EEG to be pathological in all cases.

For each of the 10 stroke subjects, we computed th μ_i and σ_i, and compared the results to those of the 18 normal subjects discussed in Ref. [4]. In this exploratory phase, we tried various combinations of these global parameters in order to find one that separates well the two subject groups. In Fig. 3a, we show a scatter plot for all 28 subjects, expressed in terms of the composite variables $\ln(\mu_1\mu_2)$ versus $\ln(\sigma_1\sigma_2)$. Open circles represent 18 normal subjects, and filled circles represent 10 stroke subjects. The two groups are remarkably well separated, confirming the potential clinical utility of this kind of analysis. It remains to understand what is different about the α_i for the two groups, and that is the subject of future study.

We stated at the outset that our objective was to arrive at a summary statistic which cleanly separates the two groups. By noting in Fig. 3a that the two groups are separated in by a diagonal line corresponding to $\ln(\mu_1\mu_2) + \ln(\sigma_1\sigma_2) =$constant, we can define a maximally compressed summary statistic

$$S = -\ln(\mu_1\mu_2\sigma_1\sigma_2) \ , \tag{9}$$

which separates the subjects along a single parameter. In Fig. 3b, we show a histogram of the number of subjects $N(S)$ having various values of S. The open bars are for the control subjects, and the filled bars are for the stroke subjects. The separation of the two groups is striking. There is only one subject from each category overlapping at $S \approx 6.5$, indicated by a scaled bar.

What we have found is a measure S that can classify the state of the EEG time series inasmuch as the body temperature T is a measure of the general health of a person. The mathematical details involved in deriving S are analogous to the mechanical and chemical details in the construction of a thermometer. But the utility of S and T transcends the complications associated with the manufacturing of those devices. With further validation, and a better understanding of the range of possible parameters in normal subjects under a variety of conditions, the measure S could prove useful for clinical stroke detection.

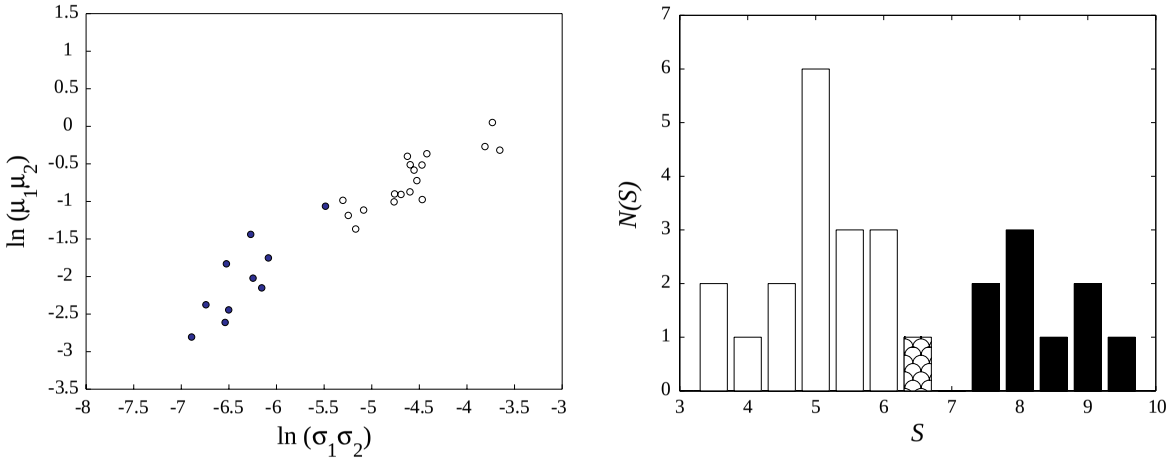

Figure 3: Separation of normal and stroke subjects. (a) Plots of $\ln(\mu_1\mu_2)$ versus $\ln(\sigma_1\sigma_2)$ for 18 normal subjects (open circles) and 10 stroke subjects (filled circles). (b) Plots of the number of subjects $N(S)$ with value S for 18 normal subjects (open bars) and 10 stroke subjects (filled bars). The scaled bar in (b) represents an overlap of one subject from each group.

4 Conclusions

We have developed a novel approach for quantifying the variability of two dynamical measures, i.e., the α_i, across 128 scalp electrodes. The approach ignores spatial topography in favor of considering the moments of the statistical distributions of the α_i. This has several advantages. First, it disentangles the analysis from the EEG inverse problem. Second, it shifts the emphasis from local to global behavior. This reveals fundamental simplicities of the data, i.e., power-law scaling behavior of the moments, not previously recognized. Third, it provides concise summary statistics which accomplish a long-standing objective of reducing the enormous amount of data arising from dense-array EEG, which in turn facilitates comparisons across subjects. Conveniently, the computational demands are minimal, making the technique suitable for rapid data processing and clinical applications.

The global parameters derived here were shown to be capable of distinguishing normal from stroke subjects. One possible conclusion is that stroke, although focal in terms of a reduction in cerebral blood flow, may have global effects on EEG dynamics. This is certainly plausible given the existence of long-range fibers connecting distant cortical regions, some of which are no longer

functional when even a small stroke occurs. Such remote effects have been suggested in previous studies based upon Fourier analysis [5]. The next step is to verify this interpretation. Why does the measure S separate the two subject groups so well? Is the key to stroke detection truly global brain dynamics, or are these global parameters merely sensitive to focal anomalies, which would suggest that further effort could perhaps also localize the stroke-affected brain area? These questions are the subject of future research.

Acknowledgements

We thank Dr. Phan Luu and Prof. Don Tucker for supplying the EEG data for our analysis. We have also benefited from the computational assistance of Wei He. This work was supported, in part, by the National Institutes of Health under Grant Nos. NS-38829 and NS-27900, and by the U.S. Department of Energy under Grant No. DE-FG03-96ER40972.

References

[1] Ferree, T. C. and R. C. Hwa. Power-law scaling in human EEG: Relation to Fourier power spectrum. Submitted to: Neurocomputing, this issue.

[2] C. W. Gardiner, *Handbook of Stochastic Methods* (Springer-Verlag, Berlin, 1983).

[3] Hwa, R. C. (1990). Fractal measures in multiparticle production. Physical Review D 41: 1456-1462.

[4] Hwa, R. C. and T. C. Ferree (2002). Scaling properties of fluctuations in human electroencephalogram. Submitted to: Physical Review E.

[5] Nagata, K. (1988). Topographic EEG in brain ischemia - Correlation with blood flow and metabolism. Brain Topography 1(2): 97-106.

[6] Nunez, P. L. *Neocortical dynamics and human EEG rhythms.* (Oxford University Press, 1995).